



The enhanced π – π interactions in metallomesogens



Ta-Ming Liu, Kuan-Ting Lin, Fu-Joun Li, Gene-Hsiang Lee[†], Ming-Chou Chen^{*},
Chung K. Lai^{*}

Department of Chemistry, National Central University, & Center for Nano Science Technology, UST, Chung-Li 32054, Taiwan, ROC

ARTICLE INFO

Article history:

Received 20 July 2015

Received in revised form 29 August 2015

Accepted 3 September 2015

Available online 16 September 2015

Keywords:

Metallomesogens

Salicylaldimines

Smectic

Nematic

ABSTRACT

Two new series of mesogenic palladium complexes **1a–b** derived from salicylaldimines containing phenyl or naphenyl moiety were prepared, characterized and their mesomorphic properties investigated. Two single crystallographic structures of mesogenic **1a** ($n=4$) and nonmesogenic **1b** ($n=3$) were determined by X-ray analysis; both crystals crystallize in a triclinic space group P1. The geometry at both palladium atoms was nearly square planar. All Schiff bases **2a–b** and palladium complexes **1a–b** exhibited mesomorphic properties. However, the formation of mesophases was sensitive to terminal naphthalyl and phenyl group. Compounds **2a** formed N or/and SmC phases and compounds **2b** exhibited N or/and SmC phases. In contrast, palladium complexes **1a** formed N or N/SmC phases and complexes **1b** exhibited N, N or/and SmC phases. Compounds **1b** have a higher clearing temperature than those of **1a** by a $\Delta T_{cl}=35.4$ – 14.8 °C. An improved mesomorphic behavior observed in compounds **1b** was attributed to the H-bonds and π – π interaction.

© 2015 Elsevier Ltd. All rights reserved.

1. Introduction

Novel metallomesogens^{1–3} generated by incorporation of metal ions into organic moieties have been successfully applied during the past decades. Metal ions played an important role in the resulting mesomorphic properties, and metallomesogens might be obtained by non-mesogenic organic ligands. In contrast, the mesomorphic properties may be totally lost upon incorporation of a metal ion. A precise prediction of phase behavior has not been feasible. One of the major challenges in the design of mesogenic materials is to understand the molecular interaction induced in the liquid crystal states. This is particularly crucial in the field of mesogenic materials. Too strong or too weak an interaction force often resulted in the formation of a solid or liquid state. On the other hand, the study of structure-property relationship is needed since they often provide much microscopically and/or macroscopically useful information in the formation of mesophases.

Salicylaldimines^{4–8} were probably one of the most ligands employed to generate metallomesogenic materials due to their synthetic versatilities and abilities to the transition metal ions. When structures were properly designed, some such derivatives were highly π -conjugated systems, useful in catalytic, photo-physical and supramolecular applications.^{9,10} A few similar

metallomesogens^{11–13} **I–II** (Fig. 1) were previously prepared and their mesomorphic properties studied. Complexes **Ia**, **IIa** formed smectic phases, while complexes **Ib**, **IIb** exhibited columnar phases. A phase change was often possible by altering their length-to-width ratios (or aspect ratios) of the prepared molecules. However, a lack of single crystallographic data of particular molecules was not able to allow us to understand its microscopic information on the formation of observed mesophases.

In this work, two new series of mesogenic palladium complexes derived from salicylaldimines were prepared, characterized and their mesomorphic properties were studied. Two single crystallographic structures of mesogenic **1a** ($n=4$) and nonmesogenic **1b** ($n=3$) were determined by X-ray analysis in order to understand the relationship of structure-property. A terminal moiety containing naphthalyl and phenyl groups was incorporated to enhance their intermolecular interactions. Single crystallographic data indicated that CH– π or/and π – π interactions were responsible to the formation of mesophases. Compounds **2a** formed N or/and SmC phases, and compounds **2b** exhibited N or/and SmC phases. In contrast, palladium complexes **1a** formed N, or/and SmC phases and complexes **1b** exhibited N, N and SmC phases.

2. Results and discussion

2.1. Synthesis and characterization

All Schiff bases **2a–b** and palladium complexes **1a–b** were summarized in Scheme 1 and Scheme 2. The compounds **2a–b**

^{*} Corresponding authors. Tel.: +886 0 3 4259207; fax: +886 0 3 4277972; e-mail address: cklai@cc.ncu.edu.tw (C.K. Lai).

[†] Instrumentation Center, National Taiwan University, Taipei 10660, Taiwan, ROC.

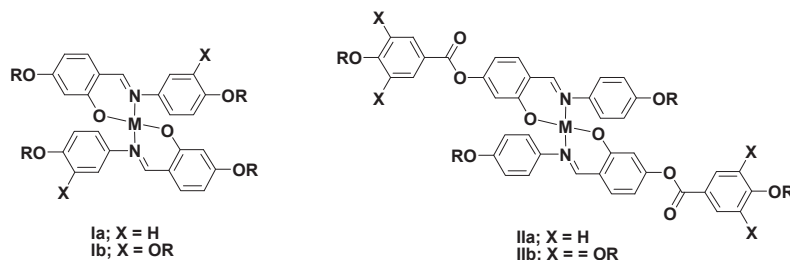
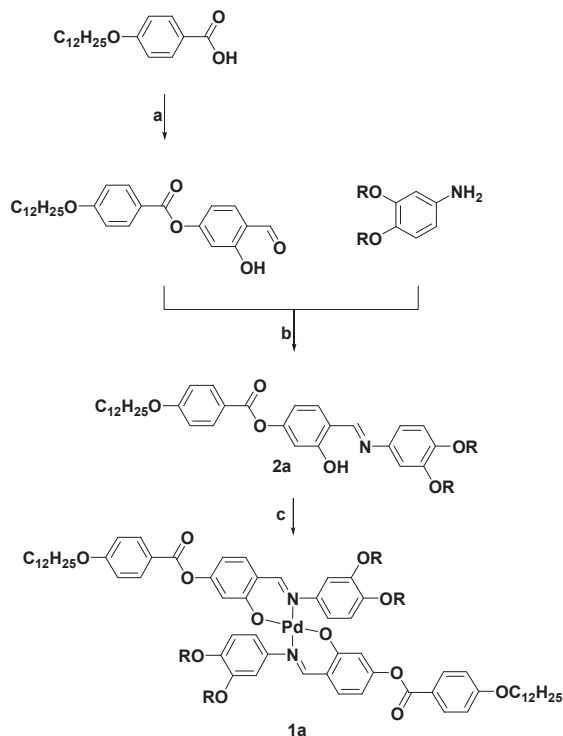


Fig. 1. The structures of known metallomesogens.

were similarly prepared from our previous procedures. The condensation reactions of appropriate 4-formyl-3-hydroxyphenyl 4-(dodecyloxy)benzoate or 4-formyl-3-hydroxyphenyl 6-(dodecyloxy)-2-naphthoate and 3,4-dialkoxyphenylamines in refluxing ethanol gave the compounds **2a** and **2b**, respectively. Both compounds isolated as yellow solids were obtained after recrystallization from THF/CH₃OH. The ¹H and ¹³C NMR spectroscopy in CDCl₃ were used to characterize all intermediates. For instance, two characteristic singlet peaks occurred at δ 8.57–8.59 and 13.63–13.78 ppm, assigned for imine–CH=N and phenolic–OH groups were observed for compounds **2a**. In contrast, these two singlet peaks were slightly shifted to δ 8.59–8.60 and 13.37–13.72 ppm for compounds **2b**. The phenolic peak –OH was barely observed due to the formation of intramolecular H-bonds with imine–N groups. The palladium complexes were obtained by the reactions of appropriate palladium (II) acetate in refluxing ethanol. The palladium complexes were isolated as light–orange compounds and the elemental analysis was used to confirm the purity of the metal complexes.



Scheme 1. Reactions and reagents. (a) 2,4-Dihydroxybenzaldehyde (1.0 equiv), DCC, DMAP in dry CH₂Cl₂, 24 h, 40%. (b) 3,4-dialkoxy-1-amino benzene (1.0 equiv), CH₃COOH (drops) in C₂H₅OH, 24 h, 75%. (c) Pd(OAc)₂ (0.5 equiv), refluxing in C₂H₅OH, 2 h, 80%.

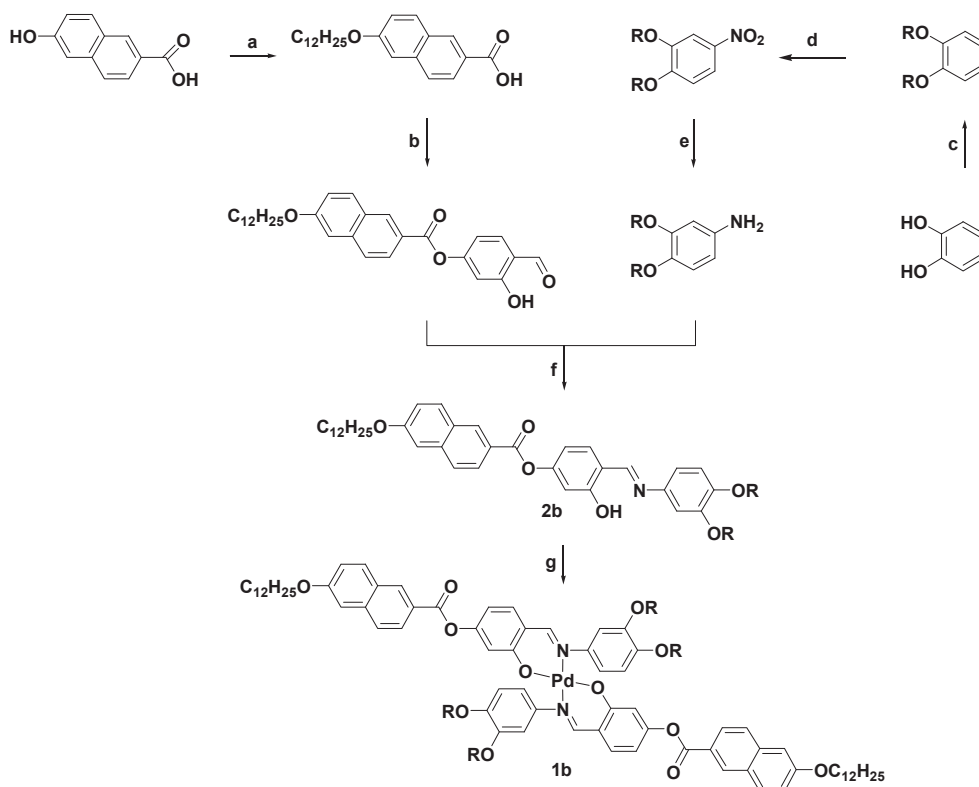
2.2. Single crystal structures of palladium complexes derived from (*E*)-4-(((3,4-dibutoxy phenyl)imino)methyl)-3-hydroxyphenyl-4-(dodecyloxy)benzoate and (*E*)-4-(((3,4-dipropoxyphenyl)imino)methyl)-3-hydroxyphenyl-2-naphthoate

In order to understand the correlation between the molecular structures and the formation of mesophases, two single crystals of palladium complexes **1a** ($n=4$) and **1b** ($n=3$) were obtained and their single crystallographic data were investigated. Light orange crystals suitable for X-ray diffraction analysis were slowly grown from CH₂Cl₂ at room temperature. Fig. 2 shows the molecular structures with the atomic numberings, and Table 1 listed the crystallographic and structural refinement data for the two molecules.

The crystal **1b** crystallizes in the triclinic space group *p*1, with $a=9.1373$ (1) Å, $b=10.9230$ (1) Å, $c=13.5756$ (2) Å, and $Z=1$. The geometry at palladium center is nearly square planar. The two angles of N (1)–Pd–O (1)# and N (1)–Pd–O are of 88.99 (5)° and 91.01 (5)°, which show almost an ideal angle of 90° expected for a square-planar geometry. The overall structure of **1b** was twisted and the molecular length was 26.9 Å (atoms C15–C15). The two dihedral angles of ca. ~84.9° (defined with N1–O1–Pd–O1–N1 and C19–C24) and ca. ~76.3° (with N1–O1–Pd–O1–N1 and naphthalene ring) were larger than those of crystal **1a**. The larger dihedral angles were probably attributed to intramolecular CH–π interactions and intermolecular H-bonds in the crystal **1a**. In contrast, the crystal **1a** crystallizes in the triclinic space group *p*1, with $a=9.1762$ (2) Å, $b=10.2898$ (2) Å, $c=21.4015$ (5) Å, and $Z=1$. The geometry at palladium center is also slightly twisted square planar. The two angles of N (1)–Pd–O (1)# and N (1)–Pd–O are of 88.42 (5)° and 91.58 (5)°. The overall structure of **1a** was not planar and also twisted. The molecular length was ca. 54.6 Å (C32–C32). Two dihedral angles of 60.9° and 53.5° between the core plane (N1–O1–Pd–O1–N1) and left phenyl (C15–C20) and right phenyl rings (C9–C14) were measured. Important bond distances and bond angles of two crystals are given in Table 2.

A weak intramolecular CH–π interaction, shown in Fig. 3, with a length of 3.69 Å was observed in crystal **1a**, whereas, there was no intramolecular interaction in crystal **1b**. On the other hand, a few intermolecular forces were observed in both crystal lattices; H-bonds, CH–π interaction and offset π–π interaction. Fig. 4 showed the intermolecular H-bonds in both crystal **1a**, all with a length ranged in 2.64–2.67 Å. Compared to crystal **1a**, no intramolecular force in crystal **1b** was observed. This might be the reason why crystal **1b** has a larger dihedral angle. In fact, compounds **1b** have improved mesomorphic behavior than compounds **1a**.

In contrast, intermolecular interactions in crystal **1b** were also observed. On the same layer, molecules were orderly arranged by H-bonds (H24A ... O2=2.52 Å) and H–Pd bonds (H10A ... Pd=2.81 Å). On the above and below layers, molecules were interacted by intermolecular CH–π interaction (C–H27A ... π=3.94 Å). This probably was the reason why the phenyl ring



Scheme 2. Reactions and reagents. (a) $C_{12}H_{25}Br$ (2.1 equiv), KOH (1.1 equiv), refluxing in C_2H_5OH/H_2O , 48 h, 88%. (b) 2,4-Dihydroxybenzaldehyde (1.0 equiv), DCC, DMAP in dry CH_2Cl_2 , 24 h, 62%. (c) RBr (2.1 equiv), KOH/KI, refluxing in acetone, 48 h, 80%. (d) HNO_3 (1.2 equiv), H_2SO_4 (drops), stirred in CH_2Cl_2 , 24 h, 86%. (e) H_2NNH_2 (1.2 equiv), Pd/C (0.1 equiv), refluxing in C_2H_5OH , 24 h, 82%. (f) CH_3COOH (drops), refluxing in C_2H_5OH , 24 h, 78%. (g) $Pd(OAc)_2$ (0.5 equiv), refluxing in C_2H_5OH , 2 h, 75%.

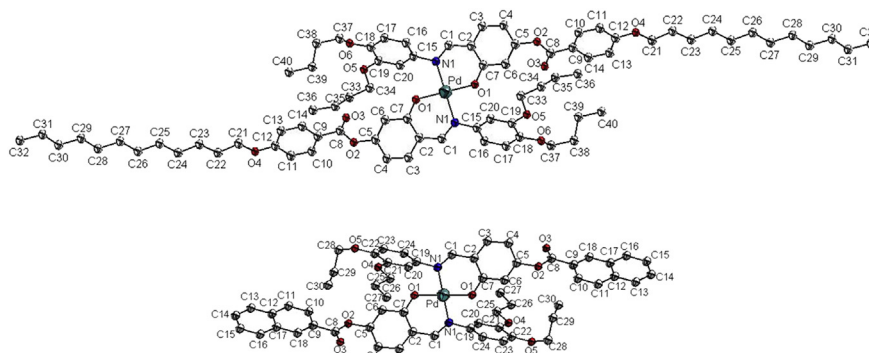


Fig. 2. Two ORTEP plots are shown. The thermal ellipsoids of the non-hydrogen atoms are drawn at the 50% probability level. Top plot: **1a** ($n=4$), and a molecular length (C32–C32)=54.6 Å, molecular width (C4–C17)=7.56 Å, molecular aspect ratio=7.22. Bottom plot: compounds **1b** ($n=3$), and a molecular length (C15–C15)=26.9 Å, molecular width (C4–C17)=6.60 Å, molecular aspect ratio=4.08.

(C19~C24) was almost perpendicular to the core plane (N1–O1–Pd–O1–N1), which was favorable to the formation of mesomorphic properties (see Table 3). However, when the phenyl groups were extended to corresponding naphthalyl groups, from **1a** to **1b**, the stronger π – π interactions might not be the only parameter. The aspect ratio between flexible alky chains and the rigid cores was also changed. Fig. 5 showed the molecular arrangements in **1a** ($n=4$) and **1b** ($n=3$).

2.3. Mesomorphic behavior

The liquid crystalline behavior of ligands **2a–b** were characterized and studied by differential scanning calorimetry (DSC) and polarized optical microscope (POM). The phase transitions and thermodynamic data are summarized in Table 4. All compounds **2a**

were mesogenic and exhibited nematic/smectic C or smectic C phases. Their clearing temperatures remained at $T_{cl}=104.5$ – 114.1 °C on the heating process, and the mesophase temperature decreased slightly with carbon chain lengths; $\Delta T_{mesophase}=42.7$ ($n=4$) >22.5 ($n=12$) >11.8 °C ($n=16$) on the cooling process. All derivatives **2a** exhibited a monotropic behavior. Under optical microscope they all exhibited typical Schlieren textures of four or/and two brushes (Fig. 6). Furthermore, the nematic phase showed slightly homeotropic domains, whereas, the smectic C phases showed no homeotropic textures. The transition enthalpies of N-to-Iso transitions were relatively small, $\Delta H=0.82$ – 1.17 kJ/mol. On the other hand, all derivatives **2b** exhibited improved mesomorphic properties. The shorter derivative ($n=3$) showed monotropic smectic C phases, while all other compounds **2b** ($n=7, 8, 10, 12, 14, 16$) showed enantiotropic behavior. The four shorter derivatives ($n=3, 7, 8, 10$)

Table 1
Crystallographic and experimental data for compounds **1a** ($n=4$) and **1b** ($n=3$)

Compds	1a ($n=4$)	1b ($n=3$)
Empirical formula	C ₈₀ H ₁₀₈ N ₂ O ₁₂ Pd	C ₆₀ H ₅₆ N ₂ O ₁₀ Pd
Formula weight	1396.08	1071.47
T/K	150 (1)	150 (1)
Wavelength/ \AA	0.71073	0.71073
Crystal system	Triclinic	Triclinic
Space group	P1	P1
$a/\text{\AA}$	9.1762 (2)	9.1373 (1)
$b/\text{\AA}$	10.2898 (2)	10.9230 (1)
$c/\text{\AA}$	21.4015 (5)	13.5756 (2)
$\alpha/^\circ$	93.7538 (10)	85.8894 (8)
$\beta/^\circ$	98.2746 (11)	86.5565 (7)
$\gamma/^\circ$	111.4061 (11)	66.8850 (8)
$U/\text{\AA}^3$	1846.44 (7)	1242.20 (3)
Z	1	1
$F(000)$	744	556
$D_c/\text{Mg m}^{-3}$	1.256	1.432
Crystal size/ mm^3	0.40×0.40×0.17	0.40×0.22×0.10
Range for data collection/ $^\circ$	1.94–27.5	1.50–27.5
Reflection collected	26,162	23,978
Data, restraints, parameters	8440/0/430	5703/0/332
Independent reflection	8440 [$R_{\text{int}}=0.0464$]	5703 [$R_{\text{int}}=0.0362$]
Final $R1$, $wR2$	0.0342, 0.0785	0.0304, 0.0776

Table 2
Crystallographic and experimental data for compounds **1a** and **1b**

Compds	1a ($n=4$)	1b ($n=3$)
Pd–O (1)	1.980 (10)	1.978 (12)
Pd–O(1)#1	1.980 (10)	1.978 (12)
Pd–N(1)	2.027 (13)	2.014 (15)
Pd–N(1)#1	2.027 (13)	2.014 (15)
O(1)–C(7)	1.310 (18)	1.306 (2)
N(1)–C(1)	1.300 (2)	1.298 (2)
C(1)–C(2)	1.431 (2)	1.437 (2)
N(1)–Pd–O(1)#	88.42 (5)	88.99 (5)
N(1)–Pd–O(1)	91.58 (5)	91.01 (5)
N(1)#–Pd–O(1)#	91.58 (5)	91.01 (5)
N(1)#–Pd–O(1)	88.42 (5)	88.99 (5)
O(1)–Pd–O(1)#	180.0 (8)	180.0 (8)
N(1)#–Pd–N(1)	180.0 (9)	180.0 (14)
C(7)–O(1)–Pd	126.9 (10)	124.3 (11)

Symmetry transformations used to generate equivalent atoms. #1– x , $-y$, $-z$.

showed both nematic and smectic C phases, whereas, all other longer derivatives ($n=12, 14, 16$) exhibited only smectic C phases. The clearing temperatures were all slightly higher than those of derivatives **2a** by ca. $\Delta T_{\text{cl}}=17.1$ ($n=16$)– 30.0 $^\circ\text{C}$ ($n=8$). However, the temperature range of mesophases for derivatives **2b** were slightly wider than those of compounds **2a**, ca. at $\Delta T_{\text{mesophase}}=62.5$ ($n=3$)– 27.2 $^\circ\text{C}$ ($n=16$) on cooling process. A larger core size incorporated with a naphthalene group in compounds **2b** than that of compounds **2a** was apparently favorable to the formation of mesophases. More π – π or CH– π interactions induced or/and enhanced by naphthalene moiety was attributed to the better mesomorphic properties. An enthalpy of $\Delta H=0.40$ – 1.53 and $\Delta H=3.02$ – 8.25 kJ/mol for N→*Iso* and SmC→N (or SmC→*Iso*) were obtained. A similar textures for nematic and smectic was observed under optical microscope.

Palladium complexes derived from compounds **2a–b** were prepared and studied. All Pd compounds **1a–b** were truly mesogenic (see Table 5). Compound **1a** ($n=3$) was the only one, kinetically unstable, showing monotropic nematic phase. All complexes **1a** have much higher clearing temperatures than those their ligand precursors **2a** by $\Delta T_{\text{cl}}=85.5$ ($n=4$)> 41.8 ($n=10$)> 32.1 $^\circ\text{C}$ ($n=16$), which was due to their larger sizes or more rigid cores. The clearing temperature were ranged from $T_{\text{cl}}=195.2$ ($n=4$)– 138.1 $^\circ\text{C}$

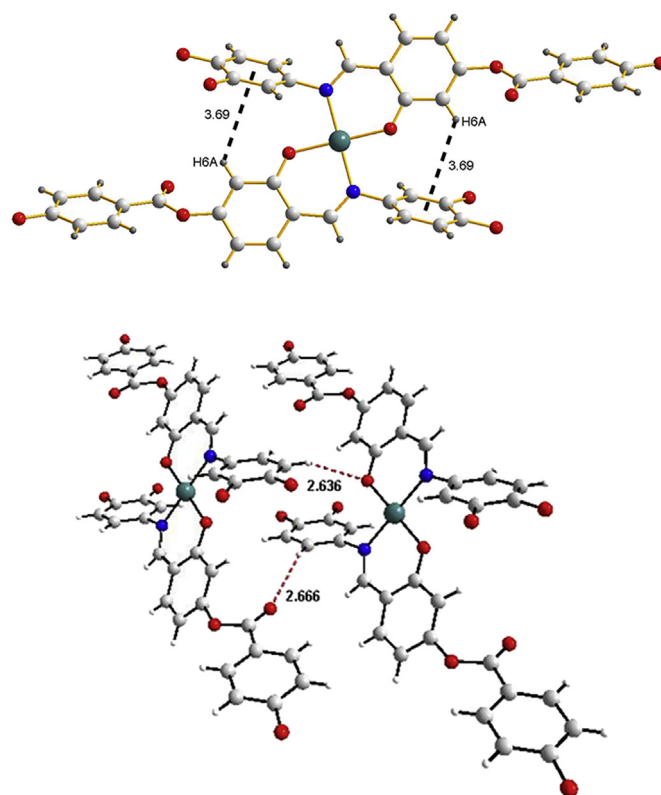


Fig. 3. Top plots: two intramolecular CH– π interactions in crystal **1a** ($n=4$); the distances between C–H27A ... π were ca. 3.69 Å. Bottom plots: a correlated structure induced by intermolecular H-bonds H17A ... O1=2.64 Å and H16A ... O3=2.67 Å, observed in **1a**.

($n=16$), and they also slightly decreased with carbon lengths; $T_{\text{cl}}=195.2$ ($n=4$)> 147.8 ($n=12$)> 138.1 $^\circ\text{C}$ ($n=16$) on heating process. On the other hand, the mesophase temperatures were ranged from $\Delta T_{\text{mesophase}}=47.6$ ($n=4$)> 28.2 ($n=10$)> 16.5 $^\circ\text{C}$ ($n=16$) on the cooling process. The mesophase were identified as nematic and smectic C phases. Under microscope, a focal–conic or Schlieren texture, as characteristic textures of nematic or smectic C phases was observed. In contrast, all complexes **1b** showed enantiotropic behavior (Fig. 7), and they all have higher clearing temperatures than those of complexes **1a** by $\Delta T_{\text{cl}}=35.4$ ($n=8$)– 14.8 $^\circ\text{C}$ ($n=14$). The clearing temperature decreased with carbon length, $T_{\text{cl}}=255.2$ ($n=3$)– 159.0 $^\circ\text{C}$ ($n=14$). Interestingly, the temperature range of compounds **1b**, $\Delta T_{\text{mesophase}}=64.6$ ($n=16$)– 135.2 ($n=8$) on the cooling process was much wider than those of compounds **1a** (Fig. 8). This wider mesophase temperature in compounds **1b** over than **1a** might be attributed to the enhanced π – π interactions resulted from incorporated naphthalene groups. The central core size and geometry structure at palladium atom in both compounds **1a** and **1b** were similar, however, the more π – π interactions favored the molecular packing in solid or LC states, facilitating or/and stabilizing the formation of the mesophases. The typical textures described as Schlieren domains for nematic and smectic C phases were also confirmed. The geometry at palladium atoms in both complexes **1a–b** was close to perfect square plane. However, a slightly twisted structure and a larger dihedral angle in crystal **1b** than those of **1a** were obviously more favorable to stabilize the mesophases.

The thermal stability of compounds **1–2** (all $n=10$) was also performed by thermogravimetric analyses (TGA) under nitrogen atmosphere, shown in Fig. 9. All four compounds showed good thermal stability at a temperature below ca. $T=331.7$ $^\circ\text{C}$, with

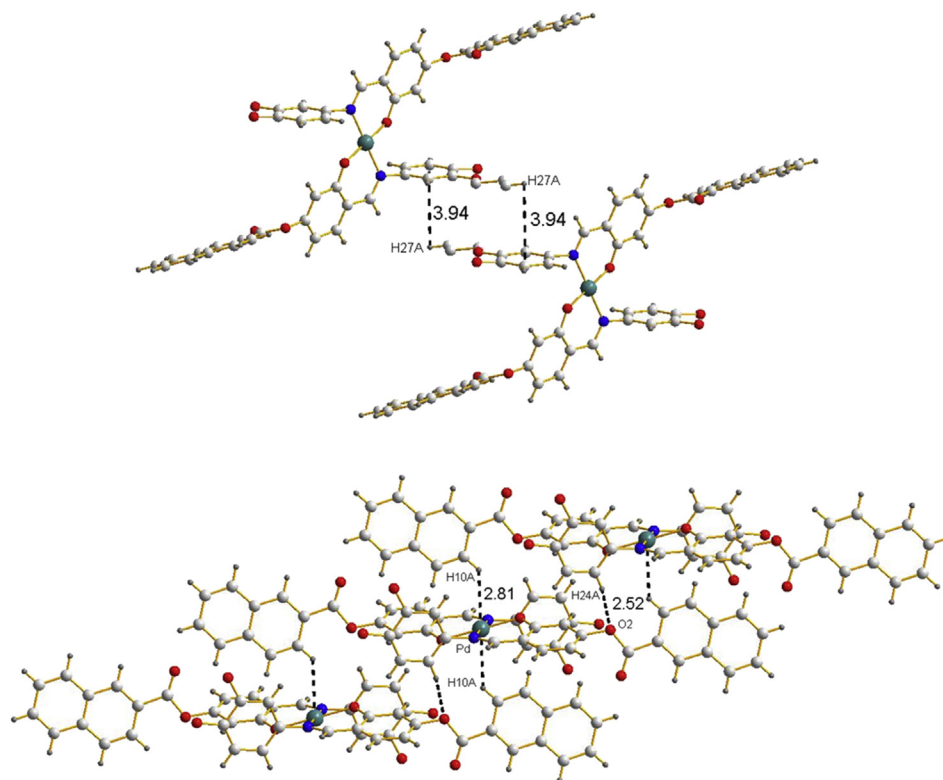


Fig. 4. A correlated structure induced by intermolecular H-bonds, H–Pd bonds and the intermolecular CH– π interactions observed viewed from different axes in **1b** ($n=3$). Top plot: C–H27A ... $\pi=3.94$ Å, and bottom plot: H24A ... O2=2.52 Å, H10A ... Pd=2.81 Å.

Table 3

A summary of molecular interactions observed in **1a** ($n=4$) and **1b** ($n=3$)

Comps	1a ($n=4$)	1b ($n=3$)
CH– π interactions	C–H6A ... $\pi=3.69$ Å	C–H27A ... $\pi=3.69$ Å
No. of H–bonds	2	1
Bond distance, angles	O1–H17A=2.64 Å \angle C17–H17A–O1=154.9° O3–H16A=2.67 Å \angle C16–H16A–O3=145.6°	O2–H24A=2.52 Å \angle C24–H24A–O2=162.2°
H–Pd bondings	—	Pd–H10A=2.81 Å

a relative thermal stability of **1a**>**2a**>**1b**>**2b**. The decomposition temperatures for a 5% weight loss were listed in Table 6. The relative order of decomposition temperature of compounds was not quite consistent with the DSC data ($T_{cl}=\mathbf{1b}>\mathbf{1a}>\mathbf{2b}>\mathbf{2a}$) of these two compounds. The clearing temperature of compound **1b** ($n=10$) was the highest at $T_{cl}=184.1$ °C, whereas, the compound **2a** was the lowest clearing temperature at $T_{cl}=114.1$ °C among the series.

2.4. Powder X-ray diffractions and packing arrangements

Variable-temperature powder XRD diffraction experiments were performed to confirm the structure of the mesophases of four compounds **2a–b** ($n=10$) and **1a–b** ($n=10$), and a summary of diffraction data was listed in Table 7. For example, for compounds **2a** ($n=10$) at 100 °C a diffraction pattern with one strong peak at 30.9 Å was observed, as shown in Fig. 10. One diffraction peak at lower angles was typically characteristics of layer structures observed for a SmC phase. A diffraction peak of nematic phase for compound **2b** ($n=10$) at higher temperature was not possible due to its quite narrow range (ca. $\Delta T_N=2.8$ °C) of mesophase temperature. In contrast, a slightly larger d-spacing of 32.1 Å at 130 °C, as expected for larger or longer structures of compound **2b** ($n=10$). A

broad halo peak appeared at ca. 4.49 and 4.80 Å was observed for two compounds. All molecules were tilted arranged in smectic phases. The molecular lengths of compounds **2a** ($n=10$) and **2b** ($n=10$) were estimated as 45.6 Å and 48.1 Å, respectively, by MM2 model. This might indicate that all molecules were tilted or/and the alkoxy carbon chains were interdigitated in SmC phases.

On the other hand, both palladium complexes **1a–b** ($n=10$) formed enantiotropic nematic at higher temperature and smectic phases at lower temperature. On XRD plots, a similar diffraction pattern with a d-spacing of 29.9 Å at 150 °C, and 28.2 Å and 14.1 Å at 140 °C for compound **1a** ($n=10$) was obtained, which were assigned as a nematic and a smectic of indices 001, and 002. A slightly longer d-spacing in nematic (~ 29.9 Å) was expected than that in layered structure (~ 28.2 Å) due to tilted molecular arrangements in SmC phase. Further, a diffraction pattern with a d-spacing of 29.9 Å at 170 °C, and 28.9 Å and 14.4 Å at 145 °C for compound **1b** ($n=10$) was obtained. A broad halo peak appeared at ca. 4.72 and 4.63 Å was observed for two these compounds. The intensities of diffraction peaks in nematic phases were all much weaker than those in smectic phases.

3. Conclusions

Two new series of mesogenic palladium complexes **1a–b** derived from salicylaldehydes containing terminal phenyl or naphenyl moiety were prepared, characterized and their mesomorphic properties were investigated. Two single crystallographic structures of compounds **1a** ($n=4$) and **1b** ($n=3$) were determined by X-ray analysis. The formation of mesomorphic properties in palladium complexes was found to be sensitive to the intermolecular interactions of CH– π interactions and H-bonds. All Schiff bases **2a–b** and palladium complexes **1a–b** exhibited mesomorphic properties. Compounds **1b** have a higher clearing temperature than

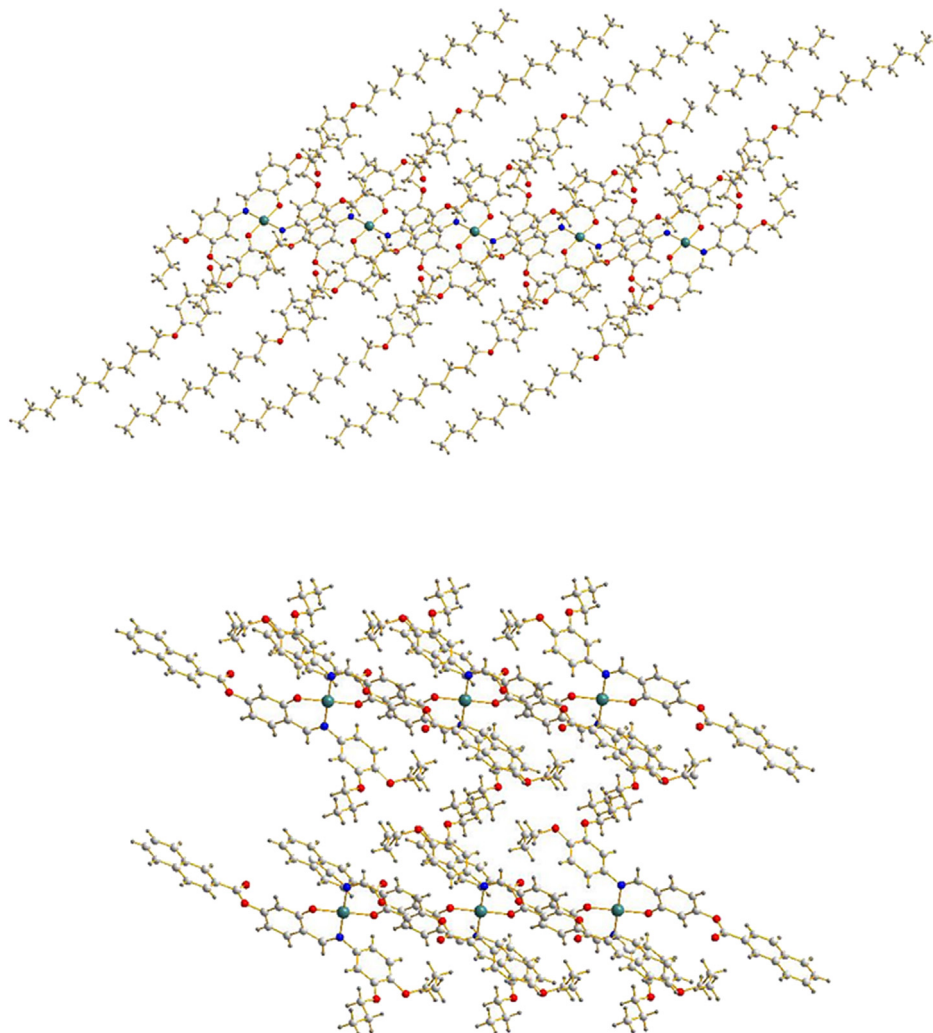


Fig. 5. Molecular arrangements in **1a** ($n=4$) and **1b** ($n=3$).

those of **1a** by a $\Delta T_{cl}=35.4\text{--}14.8$ °C. Both H-bonds and/or $\pi\text{--}\pi$ interactions might be quite important factors in inducing the mesomorphic properties observed in such type of metallomesogens. Future work might focus more on other transition metals.

4. Experimental section

4.1. General materials and methods

All chemicals and solvents were reagent grade from Aldrich Chemical Co., and solvents were dried by standard techniques. ^1H and ^{13}C NMR spectra were measured on a Bruker DRS-300. DSC thermographs were carried out on a Mettler DSC-822 and calibrated with a pure indium sample. All phase transitions are determined by a scan rate of 10.0 °C/min. Optical polarized microscopy was carried out on Zeiss Axioplan 2 equipped with a hot stage system of Mettler FP90/FP82HT. The UV-vis absorption and fluorescence spectra were obtained using a Jasco V-530 and Hitachi F-4500 spectrometer. Elemental analyses were performed on a Heraeus CHN-O-Rapid elemental analyzer. The powder diffraction data were collected from the Wiggler-A beam line of the National Synchrotron Radiation Research Center (NSRRC) with a wavelength of 1.3263 Å. The powder samples were charged in Lindemann capillary tubes (80 mm long and 0.01 mm thick) from Charles Supper Co. with an inner diameter of 1.0 mm. The

compounds of 1,2-dialkoxybenzenes, 3,4-dialkoxy nitrobenzenes and 3,4-dialkoxyaminobenzenes were prepared by literatures' procedures.

4.2. 1,2-Bis(dodecyloxy)benzene

White needle crystal, yield 80%. ^1H NMR (CDCl_3): δ 0.88 (t, 6H, $-\text{CH}_3$), 1.26–1.86 (m, 40H, $-\text{CH}_2$), 3.98 (t, 4H, $-\text{OCH}_2$), 6.88 (s, 4H, Ar-H). ^{13}C NMR (CDCl_3): δ 14.10, 22.68, 26.05, 29.36, 29.67, 31.92, 69.24, 114.07, 120.96, 149.22.

4.3. 1,2-Bis(dodecyloxy)-4-nitrobenzene

Pale yellow cotton-like crystal, yield 86%. ^1H NMR (CDCl_3): δ 0.88 (t, 6H, $-\text{CH}_3$), 1.24–1.88 (m, 40H, $-\text{CH}_2$), 4.12 (t, 4H, $-\text{OCH}_2$), 6.79 (d, 1H, Ar-H, $J=7.88$ Hz), 7.66 (s, 1H, Ar-H), 7.78 (d, 1H, Ar-H, $J=7.83$ Hz). ^{13}C NMR (CDCl_3): δ 14.12, 22.76, 25.89, 28.76, 29.47, 29.59, 30.89, 69.38, 108.21, 111.24, 117.58, 140.99, 148.67, 155.86.

4.4. 3,4-Bis(dodecyloxy)aniline

White pellet crystals, yield 82%. ^1H NMR (CDCl_3): δ 0.85 (t, 6H, $-\text{CH}_3$), 1.26–1.79 (m, 40H, $-\text{CH}_2$), 3.56 (s, 2H, $-\text{NH}_2$), 3.89 (t, 4H, $-\text{OCH}_2$), 6.23 (d, 1H, Ar-H, $J=4.66$ Hz), 6.34 (s, 1H, Ar-H), 6.78 (d, 1H, Ar-H, $J=5.68$ Hz).

Table 4
The phase transition temperatures and the enthalpies^a of compounds **2**

2a; n = 4	Cr	99.0 (51.4)		N	110.7 (1.11)	I
		66.6 (40.9)	SmC		91.9 (4.14)	
8	Cr	108.8 (5.04)		N	110.1 (0.82)	I
		81.0 (66.1)	SmC		114.1 (96.5)	
10	Cr	84.8 (75.4)		SmC	104.2 (2.81)	I
		81.7 (28.2)	SmC		106.7 (85.1)	
12	Cr	88.8 (72.1)		SmC	99.8 (7.38)	I
		88.0 (77.4)	SmC		150.8 (0.65)	
14	Cr	118.0 (38.2)		N	140.6 (1.29)	I
		85.7 (28.7)	SmC		112.0 (2.14)	
16	Cr	134.9 (5.94)		N	142.4 (1.17)	I
		122.8 (52.6)	SmC		132.6 (5.98)	
2b; n = 3	Cr	137.5 (6.33)		N	134.7 (0.40)	I
		126.9 (65.7)	SmC		135.8 (6.86)	
7	Cr	130.8 (3.02)		N	133.9 (1.18)	I
		95.5 (49.2)	SmC		130.8 (3.02)	
8	Cr	131.1 (3.68)		N	132.5 (8.28)	I
		123.9 (39.8)	SmC		131.1 (3.68)	
10	Cr	123.8 (61.2)		SmC	131.3 (8.25)	I
		102.8 (48.7)	SmC		123.8 (61.2)	
12	Cr	97.7 (61.0)		SmC	123.3 (6.64)	I
		115.8 (54.8)	SmC		97.7 (61.0)	
14	Cr	94.1 (51.5)		SmC	123.1 (5.07)	I
		118.0 (45.0)	SmC		94.1 (51.5)	
16	Cr	95.9 (64.1)		SmC	123.1 (5.04)	I
		95.9 (64.1)	SmC		95.9 (64.1)	

^a: n = carbon numbers of alkoxy chains, Cr = crystal phase; N = nematic phase; SmC = smectic C phase; I = isotropics. The temperature were determined by DSC at a scan rate of 10.0 °C.

4.5. 6-(Dodecyloxy)-2-naphthoic acid

The solution of 6-hydroxy-2-naphthoic acid (5.0 g, 0.027 mol) and KOH (3.0 g, 0.053 mol) was gently heated in 100 mL of C₂H₅OH/H₂O (10/1) for 30 min under nitrogen atmosphere. The solution was then added 1-bromododecane (13.92 g, 0.056 mol), and the mixture was refluxed for 24 h. The solution was neutralized with dilute 1.0 M HCl to pH equal to 6.0. The white solids were collected. The products isolated as white crystals were obtained after recrystallized from CH₂Cl₂/CH₃OH. Yield 88%. ¹H NMR (CDCl₃): δ 0.85–0.90 (t, 3H, –CH₃), 1.29–1.50 (m, 12H, –CH₂), 1.83–1.85 (m, 2H, –CH₂), 4.08–4.11 (t, 2H, –OCH₂), 7.14 (s, 1H, Ar–H), 7.18–7.20 (d, 1H, Ar–H, J=8.94 Hz), 7.23 (s, 1H, Ar–H), 7.73–7.75 (d, 1H, Ar–H, J=8.68 Hz), 7.83–7.85 (d, 1H, Ar–H, J=8.92 Hz), 8.04–8.06 (d, 1H, Ar–H, J=8.89 Hz), 8.59 (s, 1H, Ar–H). ¹³C NMR (CDCl₃): δ 13.91, 22.55, 26.05, 29.15, 29.28, 29.35, 31.75, 68.30, 106.72, 119.97, 121.29, 124.16, 126.05, 126.85, 127.85, 130.95, 131.80, 137.75, 159.51.

4.6. 4-Formyl-3-hydroxyphenyl 6-(dodecyloxy)-2-naphthoate

Under nitrogen atmosphere, the solution 6-(dodecyloxy)-2-naphthoic acid (2.00 g, 6.0 mmol), DCC (1.51 g, 7 mmol) and 2,4-dihydroxybenzaldehyde (0.84 g, 6.0 mmol) was dissolved in 100 mL of dry THF, and the mixture was stirred at ice-bath temperature for 30 min. The solution was then added and DMAP (0.89 g, 7 mmol) stirred at room temperature for 24 h. The solids were filtered off, and the solution was concentrated. The product

isolated as white solids was purified by column chromatography (SiO₂) eluting with hexane. Yield 62%. ¹H NMR (CDCl₃): δ 0.86–0.90 (t, 3H, –CH₃, J=6.73 Hz), 1.27–1.56 (m, 12H, –CH₂), 1.83–1.86 (m, 2H, –CH₂), 4.08–4.10 (t, 2H, –OCH₂, J=6.54 Hz), 6.91 (s, 1H, Ar–H), 6.93–6.96 (d, 1H, Ar–H, J=8.46 Hz), 7.15 (s, 1H, Ar–H), 7.20–7.22 (d, 1H, Ar–H, J=8.93 Hz), 7.60–7.62 (d, 1H, Ar–H, J=8.44 Hz), 7.77–7.79 (d, 1H, Ar–H, J=8.68 Hz), 7.85–7.87 (d, 1H, Ar–H, J=8.93 Hz), 8.08–8.10 (d, 1H, Ar–H, J=8.64 Hz), 8.65 (s, 1H, Ar–H). ¹³C NMR (CDCl₃): 14.11, 22.67, 26.10, 29.15, 29.25, 29.37, 31.83, 68.28, 106.48, 110.94, 114.18, 118.68, 120.33, 123.51, 126.00, 127.16, 127.75, 131.04, 132.06, 134.98, 137.86, 157.93, 159.70, 163.25, 164.48, 195.50.

4.7. (E)-4-(((3,4-Bis(dodecyloxy)phenyl)imino)methyl)-3-hydroxyphenyl 6-(dodecyloxy)-2-naphthoate **2b** (n = 12)

The mixture of 4-formyl-3-hydroxyphenyl 6-(dodecyloxy)-2-naphthoate (0.55 g, 1.15 mmol) and 3,4-bis(dodecyloxy)aniline (0.53 g, 1.15 mmol) was dissolved in 15 mL of hot absolute ethanol. A few drops of glacial acetic acid were added to the mixture. Then the solution was gently refluxed for 24 h. The solution was cooled and the solids were collected. The product isolated as yellow solids were obtained after recrystallization from THF/CH₃OH. Yield 85%. ¹H NMR (CDCl₃): δ 0.87 (m, 9H, –CH₃), 1.25–1.47 (m, 48H, –CH₂), 1.78 (m, 6H, –CH₂), 1.83 (m, 6H, –OCH₂CH₂), 4.01 (m, 4H, –OCH₂), 4.09 (t, 2H, –OCH₂, J=6.45 Hz), 6.88 (m, 4H, Ar–H), 6.97 (s, 1H, Ar–H), 7.16 (s, 1H, Ar–H), 7.21 (d, 1H, Ar–H, J=11.25 Hz), 7.44 (d, 1H, Ar–H, J=8.98 Hz), 8.11 (d, 1H, Ar–H, J=8.32 Hz), 8.12 (s, 1H, N=

Table 5
The phase transition temperatures and the enthalpies^a of compounds **1**

1a; n = 4	Cr			195.2 (72.3)	I	
				142.7 (60.6)		N 190.3 (0.93)
	8	Cr	131.9 (54.9)	SmC 144.2 (8.32)	N 167.5 (1.15)	I
			122.4 (59.0)	141.9 (8.73)	166.1 (1.10)	
	10	Cr	131.8 (36.9)	SmC 147.0 (8.56)	N 155.9 (1.04)	I
			126.4 (37.4)	145.2 (8.91)	154.6 (1.40)	
	12	Cr	128.6 (41.2)	SmC 144.2 (9.58)	N 147.8 (1.05)	I
122.8 (41.9)			141.5 (9.78)	145.8 (1.18)		
14	Cr		131.2 (40.4)	SmC 144.2 (12.1)	I	
			124.5 (43.4)	142.6 (12.2)		
16	Cr		124.9 (47.4)	SmC 138.1 (12.3)	I	
			120.0 (48.6)	136.5 (12.6)		
1b; n = 3	Cr			190.4 (76.1)	I	
				142.7 (60.6)		N 255.2 (1.14)
	7	Cr			129.9 (25.5)	I
					97.5 (27.1)	
	8	Cr	136.4 (46.0)	SmC 141.9 (3.06)	N 213.8 (1.42)	I
			64.5 (45.4)	137.4 (6.40)	202.9 (1.88)	
	10	Cr	122.8 (35.3)	SmC 151.2 (7.86)	N 199.7 (1.72)	I
			63.7 (15.5)	148.9 (7.29)	184.1 (1.45)	
	12	Cr	109.4 (63.7)	SmC 149.7 (9.49)	N 182.3 (1.63)	I
			65.4 (19.8)	147.7 (9.03)	167.2 (1.44)	
	14	Cr	108.3 (21.9)	SmC 147.1 (7.90)	N 166.3 (1.79)	I
			82.0 (40.5)	145.4 (8.27)	159.0 (1.23)	
	16	Cr	116.0 (75.0)	SmC 152.1 (8.19)	N 157.7 (1.48)	I
			95.5 (67.6)	151.0 (8.32)	160.8 (1.11)	

^a: n = the carbob numbers of alkoxy chains, Cr = crystal phase; N = nematic phase; SmC = smectic C phase; I = isotropics, determined by DSC at a scan rate of 10.0 °C/min.

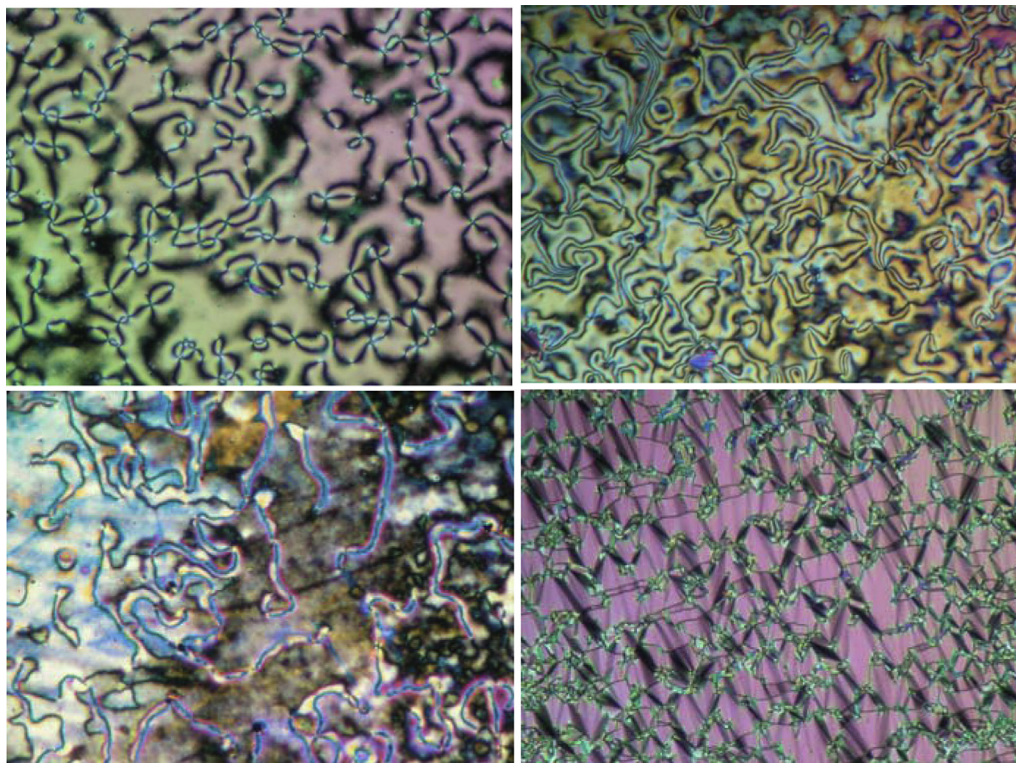


Fig. 6. Optical textures observed. N phase at 109 °C by **2a** ($n=8$, top left), SmC phase at 100 °C by **2a** ($n=8$, top right), N phase at 138 °C by **2b** ($n=8$, bottom left), SmC phase at 129 °C **2b** ($n=8$, bottom right).

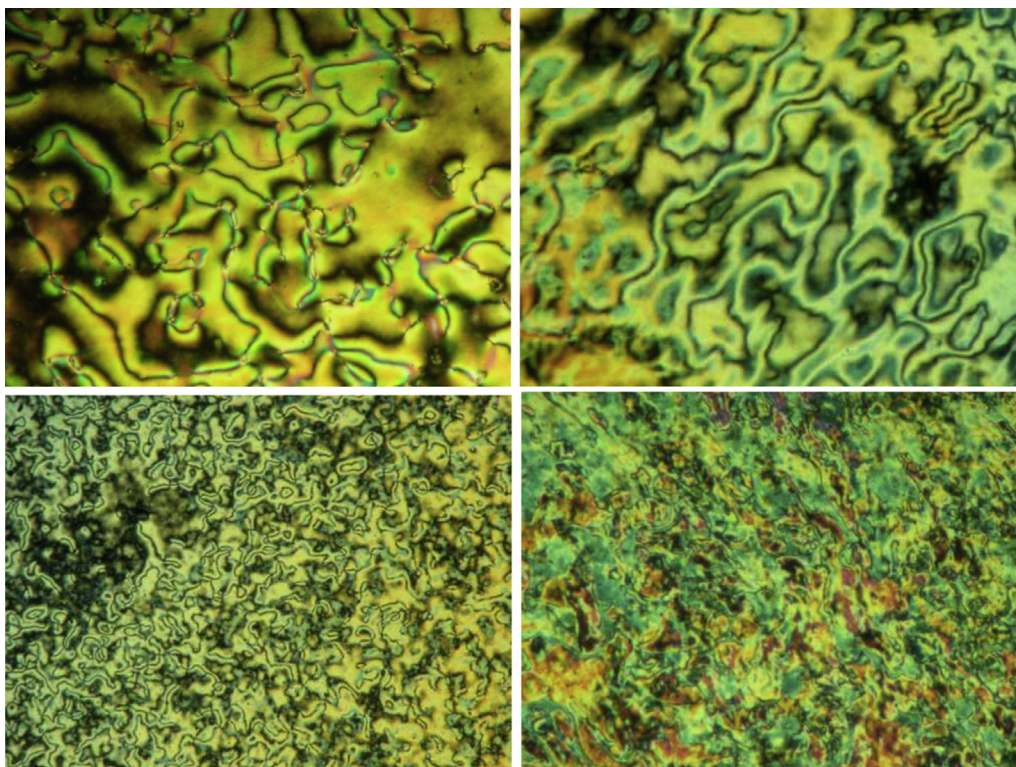


Fig. 7. Optical textures observed. N phase at 150 °C by **1a** ($n=8$, top left), and SmC phase at 125 °C **1a** ($n=8$, top right). N phase at 180 °C by **1b** ($n=8$, bottom left) and SmC phase at 100 °C by **1b** ($n=8$, bottom right).

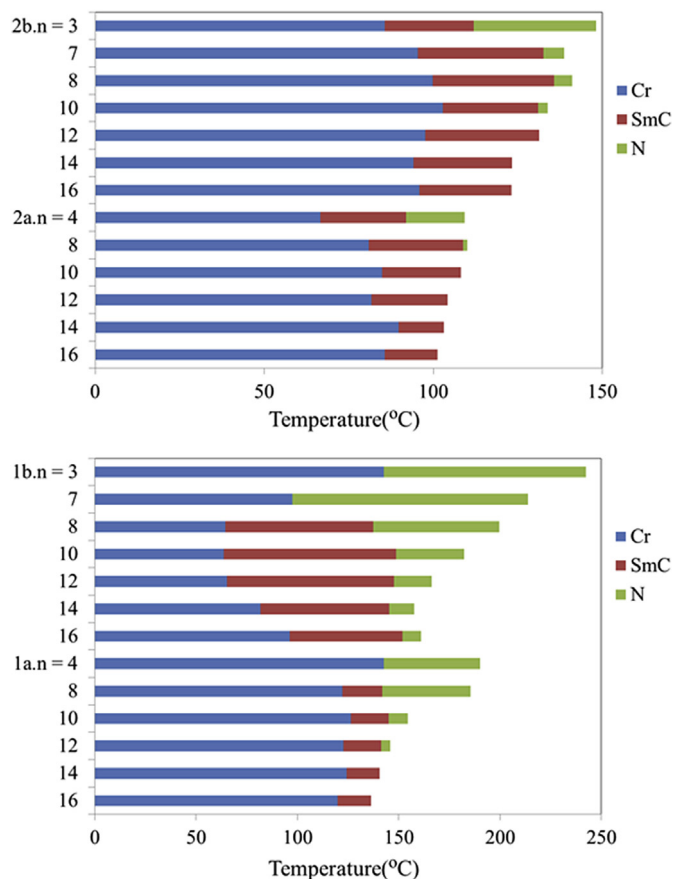


Fig. 8. Bar graphs showing the phase behavior of compounds **1–2**. All temperatures were taken on the cooling process.

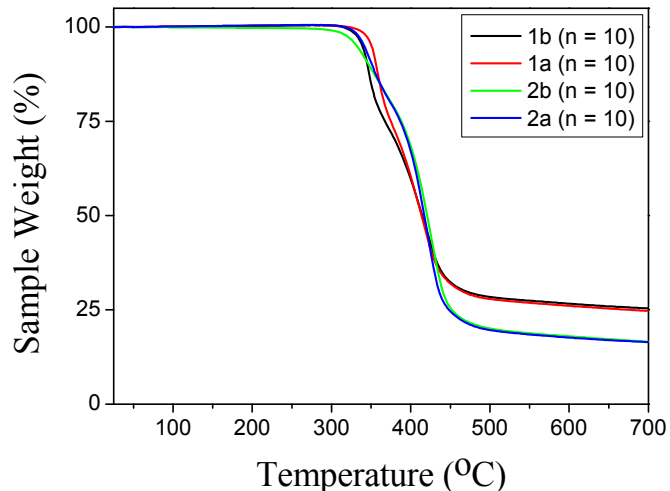


Fig. 9. The TGA thermographs of compounds **1–2** (all $n=10$) under nitrogen gas at a heating rate of 10.0 °C min⁻¹.

Table 6
The decomposition temperatures^a of compounds **1–2** (all $n=10$) by TGA analysis

Comps	T_{dec} (°C)
2b ($n=10$)	331.7
2a ($n=10$)	341.7
1b ($n=10$)	339.2
1a ($n=10$)	350.8

^a Temperatures taken with a 5% weight loss under nitrogen atmosphere.

C–H), 8.16 (s, 1H, Ar–H), 13.37 (s, 1H, Ar–OH). ¹³C NMR (CDCl₃): δ 14.13, 22.71, 26.05, 26.07, 26.14, 29.17, 29.28, 29.32, 29.36, 29.38, 29.41, 29.45, 29.60, 29.62, 29.66, 29.68, 29.73, 31.94, 68.26, 69.41, 69.61, 106.46, 107.39, 110.63, 112.99, 124.02, 126.01, 127.06, 127.80,

Table 7
Detailed indexation by powder X-ray diffractions^a for compounds **1–2**

Compd	Mesophases/temp. (°C)	<i>d</i> -Spacing obs. (Calcd.)	Miller indices
2b (<i>n</i> =10)	SmC at 130	32.07 (32.07)	001
		4.60 (br)	Halo
		30.89 (30.89)	001
2a (<i>n</i> =10)	SmC at 100	4.49 (br)	Halo
1b (<i>n</i> =10)	N at 170	29.92 (29.92)	
		4.69 (br)	Halo
	SmC at 135	28.89 (28.89)	001
		14.42 (14.44)	002
1a (<i>n</i> =10)	N at 150	4.66 (br)	Halo
		29.92 (29.92)	
		4.72 (br)	Halo
	SmC at 140	28.24 (28.24)	001
		14.07 (14.12)	002
		4.63 (br)	Halo

^a Temperature taken on the cooling process.

131.03, 131.88, 132.06, 134.98, 137.73, 148.67, 149.87, 154.67, 159.70, 162.57, 163.25, 164.95. Anal. Calcd for C₆₅H₉₄N₂O₆: C, 78.30; H, 9.75; N, 1.52. Found: C, 78.40; H, 9.74; N, 1.33.

4.7.1. (*E*)-4-(((3,4-Dipropoxyphenyl)imino)methyl)-3-hydroxyphenyl 6-(dodecyloxy)-2-naphthoate **2b** (*n*=3). Yellow solid, yield 72%. ¹H NMR (CDCl₃): δ 0.87 (t, 3H, -CH₃, *J*=6.90 Hz), 1.05 (m, 6H, -CH₃), 1.26–1.37 (m, 16H, -CH₂), 1.49 (m, 2H, -CH₂), 1.85 (m, 6H, -CH₂), 3.98 (m, 4H, -OCH₂), 4.09 (t, 2H, -OCH₃, *J*=6.54 Hz), 6.88 (m, 4H, Ar-H), 6.93 (s, 1H, Ar-H), 7.16 (s, 1H, Ar-H), 7.2 (d, 1H, Ar-H, *J*=9.20 Hz), 7.42 (d, 1H, Ar-H, *J*=8.41 Hz), 7.78 (d, 1H, Ar-H, *J*=8.66 Hz), 7.86 (d, 1H, Ar-H, *J*=9.00 Hz), 8.10 (d, 1H, Ar-H, *J*=8.02 Hz), 8.60 (s, 1H, -N=CH), 8.67 (s, 1H, Ar-H), 13.72 (s, 1H, Ar-OH) ¹³C NMR (CDCl₃): δ 0.50, 10.52, 14.14, 22.62, 22.65, 26.11, 29.17, 29.37, 29.42, 29.60, 29.63, 29.63, 29.66, 29.68, 31.94, 66.26, 70.86, 71.10, 106.46, 107.46, 110.62, 113.01, 114.22, 117.30, 120.21, 124.12, 126.11, 127.06, 127.79, 131.03, 131.88, 132.09, 137.72, 148.61, 149.81, 154.61, 159.55, 159.57, 162.56, 164.98. Anal. Calcd for C₆₅H₉₄N₂O₆: C, 75.53%; H, 8.00; N, 2.10. Found: C, 75.71; H, 7.85; N, 1.86.

4.7.2. (*E*)-4-(((3,4-Bis(heptyloxy)phenyl)imino)methyl)-3-hydroxyphenyl 6-(dodecyloxy)-2-naphthoate **2b** (*n*=7). Yellow solid, yield 80%. ¹H NMR (CDCl₃): δ 0.89 (m, 9H, -CH₃), 1.27–1.32 (m, 28H, -CH₂), 1.49 (m, 6H, -OCH₂), 1.83 (m, 6H, -CH₂), 4.02 (m, 4H, -OCH₂), 4.11 (t, 2H, -OCH₂, *J*=6.55 Hz), 6.87 (m, 4H, Ar-H), 6.93 (s, 1H, Ar-H), 7.17 (s, 1H, Ar-H), 7.14 (d, 1H, Ar-H, *J*=6.30 Hz), 7.40 (d, 1H, Ar-H, *J*=8.45 Hz), 7.77 (d, 1H, Ar-H, *J*=8.15 Hz), 7.86 (d, 1H, Ar-H, *J*=8.95 Hz), 8.11 (d, 1H, Ar-H, *J*=8.50 Hz), 8.59 (s, 1H, -N=C-H), 8.69 (s, 1H, Ar-H), 13.71 (s, 1H, Ar-OH). ¹³C NMR (CDCl₃): δ 13.94, 13.95, 22.53, 22.60, 29.09, 29.16, 29.27, 29.35, 29.41, 29.52, 29.54, 29.57, 29.60, 31.77, 31.86, 68.32, 68.62, 69.88, 76.69, 76.94, 77.19, 106.73, 107.93, 110.55, 112.86, 117.37, 120.11, 124.23, 126.07, 127.00, 127.89, 130.96, 131.79, 132.74, 137.73, 141.78, 148.86, 150.13, 154.10, 159.59, 162.60, 164.84. Anal. Calcd for C₆₅H₉₄N₂O₆: C, 76.98; H, 8.92; N, 1.80. Found: C, 77.04; H, 9.06; N, 2.26.

4.7.3. (*E*)-4-(((3,4-Bis(octyloxy)phenyl)imino)methyl)-3-hydroxyphenyl 6-(dodecyloxy)-2-naphthoate **2b** (*n*=8). Yellow solid, yield 82%. ¹H NMR (CDCl₃): δ 0.88 (m, 9H, -CH₃), 1.28–1.45 (m, 32H, -CH₂), 1.49 (m, 6H, -CH₂CH₃), 1.85 (m, 6H, -CH₂), 4.03 (m, 4H, -OCH₂), 4.11 (t, 2H, -OCH₂, *J*=6.53 Hz), 6.86 (m, 4H, Ar-H), 6.93 (s, 1H, Ar-H), 7.12 (s, 1H, Ar-H), 7.22 (d, 1H, Ar-H, *J*=6.35 Hz), 7.39 (d, 1H, Ar-H, *J*=8.45 Hz), 7.77 (d, 1H, Ar-H, *J*=8.65 Hz), 7.86 (d, 1H, Ar-H, *J*=8.95 Hz), 8.12 (d, 1H, Ar-H, *J*=8.62 Hz), 8.59 (s, 1H, -N=C-H), 8.67 (s, 1H, Ar-H), 13.67 (s, 1H, Ar-OH). ¹³C NMR (CDCl₃): δ 13.94, 22.59, 26.03, 26.96, 29.16, 29.21, 29.26, 26.33, 29.41, 29.52, 29.54, 29.57, 31.78, 31.86, 68.33, 69.64, 69.91, 106.73,

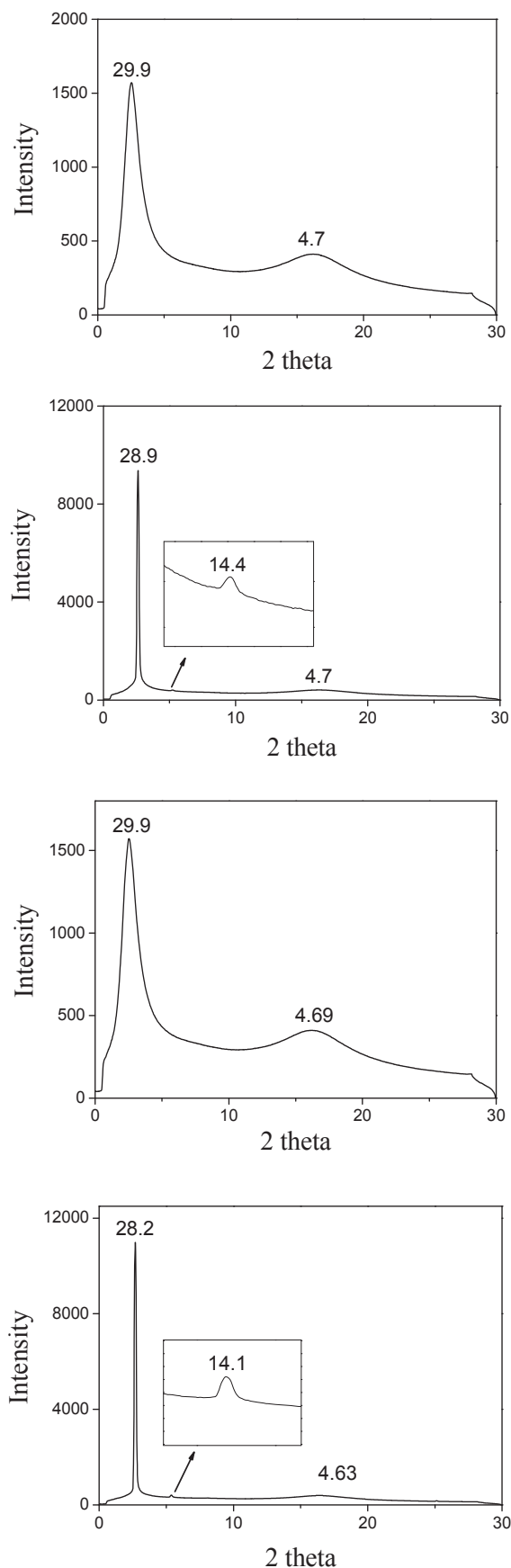


Fig. 10. The powder X-ray diffractions (from top to bottom plot) by compounds: **1a** (*n*=10) at 170 °C and **1b** (*n*=10) at 135 °C, **1a** (*n*=10) at 150 °C and **1a** (*n*=10) at 140 °C when cooled from above their clearing temperatures.

107.96, 110.55, 112.85, 113.15, 114.85, 117.38, 120.11, 124.24, 126.07, 127.00, 130.96, 131.78, 132.74, 137.74, 141.80, 148.86, 152.14, 154.70, 159.59, 159.61, 162.59, 164.83. Anal. Calcd for C₆₅H₉₄N₂O₆: C, 77.28; H, 9.10; N, 1.73. Found: C, 77.05; H, 8.81; N, 2.51.

4.7.4. (*E*)-4-(((3,4-Bis(decyloxy)phenyl)imino)methyl)-3-hydroxyphenyl 6-(dodecyloxy)-2-naphthoate **2b** (*n*=10). Yellow solid, yield 82%. ¹H NMR (CDCl₃): δ 0.88 (m, 9H, –CH₃), 1.28–1.45 (m, 40H, –CH₂), 1.49 (m, 6H, –CH₂CH₃), 1.84 (m, 6H, –CH₂), 4.03 (m, 4H, –OCH₂), 4.11 (t, 2H, –OCH₂, *J*=6.53 Hz), 6.88 (m, 4H, Ar–H), 6.93 (s, 1H, Ar–H), 7.14 (s, 1H, Ar–H), 7.40 (d, 1H, Ar–H, *J*=8.31 Hz), 7.76 (d, 1H, Ar–H, *J*=8.18 Hz), 7.86 (d, 1H, Ar–H, *J*=9.01 Hz), 8.12 (d, 1H, Ar–H, *J*=8.48 Hz), 8.60 (s, 1H, –N=C–H), 8.67 (s, 1H, Ar–H), 13.67 (s, 1H, Ar–OH). ¹³C NMR (CDCl₃): δ 13.96, 22.61, 26.04, 26.06, 29.16, 29.28, 29.35, 29.38, 29.53, 29.58, 31.86, 68.32, 69.13, 69.89, 106.72, 107.90, 110.57, 112.89, 113.14, 114.81, 120.12, 124.22, 126.08, 127.61, 127.88, 139.97, 131.80, 132.78, 137.74, 141.67, 148.87, 150.14, 159.59, 162.62, 164.83. Anal. Calcd for C₆₅H₉₄N₂O₆: C, 77.83; H, 9.45; N, 1.62. Found: C, 77.81; H, 9.53; N, 1.49.

4.7.5. (*E*)-4-(((3,4-Bis(tetradecyloxy)phenyl)imino)methyl)-3-hydroxyphenyl 6-(dodecyloxy)-2-naphthoate **2b** (*n*=14). Yellow solid, yield 81%. ¹H NMR (CDCl₃): δ 0.87 (m, 9H, –CH₃), 1.26–1.36 (m, 56H, –CH₂), 1.47 (m, 6H, –CH₂), 1.83 (m, 6H, –CH₂), 4.03 (m, 4H, –OCH₂), 4.11 (t, 2H, –OCH₂, *J*=6.45 Hz), 6.88 (m, 4H, Ar–H), 6.92 (s, 1H, Ar–H), 7.17 (s, 1H, Ar–H), 7.22 (d, 1H, Ar–H, *J*=10.28 Hz), 7.40 (d, 1H, Ar–H, *J*=8.43 Hz), 7.77 (d, 1H, Ar–H, *J*=8.16 Hz), 7.86 (d, 1H, Ar–H, *J*=8.98 Hz), 8.12 (t, 1H, Ar–H, *J*=8.58 Hz), 8.59 (s, 1H, –N=C–H), 8.67 (s, 1H, Ar–H), 13.60 (s, 1H, Ar–OH). ¹³C NMR (CDCl₃): δ 0.93, 13.95, 22.60, 26.03, 26.04, 29.16, 29.27, 29.28, 29.33, 29.35, 29.38, 29.52, 29.54, 29.58, 29.60, 26.45, 31.87, 68.32, 69.63, 69.90, 106.72, 107.93, 110.55, 112.86, 113.14, 114.84, 117.37, 120.11, 124.23, 126.07, 127.00, 127.89, 130.97, 131.77, 132.74, 137.73, 141.78, 148.78, 148.86, 150.14, 154.71, 159.60, 162.60, 164.84. Anal. Calcd for C₆₅H₉₄N₂O₆: C, 78.72; H, 10.01; N, 1.43. Found: C, 78.70; H, 9.98; N, 2.00.

4.7.6. (*E*)-4-(((3,4-Bis(hexadecyloxy)phenyl)imino)methyl)-3-hydroxyphenyl 6-(dodecyloxy)-2-naphthoate **2b** (*n*=16). Yellow solid, yield 81%. ¹H NMR (CDCl₃): δ 0.87 (m, 9H, –CH₃), 1.26–1.34 (m, 64H, –CH₂), 1.50 (m, 6H, –CH₂), 1.83 (m, 6H, –OCH₂), 4.03 (m, 4H, –OCH₂), 4.11 (t, 2H, –OCH₂, *J*=6.53 Hz), 6.88 (m, 4H, Ar–H), 6.93 (s, 1H, Ar–H), 7.17 (s, 1H, Ar–H), 7.21 (d, 1H, Ar–H, *J*=8.99 Hz), 7.40 (d, 1H, Ar–H, *J*=8.44 Hz), 7.77 (d, 1H, Ar–H, *J*=8.66 Hz), 7.87 (d, 1H, Ar–H, *J*=8.99 Hz), 8.10 (d, 1H, Ar–H, *J*=8.45 Hz), 8.59 (s, 1H, –N=C–H), 8.67 (s, 1H, Ar–H), 13.65 (s, 1H, Ar–OH). ¹³C NMR (CDCl₃): δ 13.95, 22.60, 26.04, 29.16, 29.27, 29.34, 29.36, 29.38, 29.52, 29.54, 29.58, 29.60, 29.65, 31.87, 66.32, 69.64, 69.90, 106.73, 107.94, 110.56, 112.86, 113.14, 114.84, 117.37, 120.11, 124.24, 126.07, 127.00, 130.96, 131.78, 132.74, 137.73, 141.76, 148.86, 150.14, 154.71, 159.60, 162.60, 164.83. Anal. Calcd for C₆₅H₉₄N₂O₆: C, 79.10; H, 10.25; N, 1.36. Found: C, 78.96; H, 10.26; N, 1.22.

4.8. (*E*)-4-(((3,4-Bis(dodecyloxy)phenyl)imino)methyl)-3-hydroxyphenyl 4-(dodecyloxy)benzoate **2a** (*n*=12)

Yield 78%. ¹H NMR (CDCl₃): δ 0.87 (m, 9H, –CH₃), 1.26–1.35 (m, 48H, –CH₂), 1.46 (m, 6H, –CH₂), 1.81 (m, 6H, –CH₂), 4.03 (m, 6H, –OCH₂), 6.80 (d, 1H, Ar–H, *J*=8.41 Hz), 6.86 (m, 4H, Ar–H), 6.95 (d, 2H, Ar–H, *J*=8.81 Hz), 7.37 (d, 1H, Ar–H, *J*=8.42 Hz), 8.11 (d, 2H, Ar–H, *J*=8.80 Hz), 8.57 (s, 1H, –N=C–H), 13.76 (s, 1H, Ar–OH). ¹³C NMR (CDCl₃): δ 13.94, 2.59, 22.70, 25.94, 26.02, 26.16, 29.09, 29.26, 29.28, 29.37, 29.48, 29.51, 29.63, 29.68, 31.86, 31.93, 68.24, 68.42, 69.63, 69.90, 106.44, 107.93, 110.51, 110.65, 112.29, 113.13, 114.43, 114.84, 120.15, 126.11, 127.01, 131.00, 131.82, 132.30, 132.67, 141.80, 148.83, 150.12, 159.62, 162.54, 163.41, 163.74, 164.11. Anal. Calcd for

C₆₅H₉₄N₂O₆: C, 77.28; H, 10.08; N, 1.61. Found: C, 76.82; H, 10.32; N, 1.41.

4.8.1. (*E*)-4-(((3,4-Dibutoxyphenyl)imino)methyl)-3-hydroxyphenyl 4-(dodecyloxy) benzoate **2a** (*n*=4). Yellow solid, yield 85%. ¹H NMR (CDCl₃): δ 0.86 (t, 3H, –CH₃, *J*=5.68 Hz), 0.98 (m, 6H, –CH₂), 1.00–1.25 (m, 12H, –CH₂), 1.49–1.52 (m, 6H, –CH₂), 1.82 (m, 6H, –CH₂), 4.02 (m, 2H, –OCH₂), 6.79 (d, 1H, Ar–H, *J*=8.30 Hz), 6.86 (m, 4H, Ar–H), 6.95 (d, 2H, Ar–H, *J*=8.80 Hz), 7.38 (d, 2H, Ar–H, 8.11, *J*=8.45 Hz), 8.11 (d, 1H, Ar–H, *J*=8.75 Hz), 8.58 (s, 1H, –N=C–H), 13.78 (s, 1H, Ar–OH). ¹³C NMR (CDCl₃): δ 13.04, 13.91, 14.15, 19.26, 22.72, 26.00, 29.11, 29.38, 29.61, 29.66, 31.32, 31.36, 31.94, 68.37, 69.06, 69.31, 107.43, 110.56, 112.97, 114.16, 114.35, 117.27, 121.24, 132.37, 132.86, 141.71, 148.56, 149.81, 149.81, 154.58, 162.48, 163.69, 164.43. Anal. Calcd for C₆₅H₉₄N₂O₆: C, 74.38; H, 8.58; N, 2.17. Found: C, 74.21; H, 8.39; N, 1.92.

4.8.2. (*E*)-4-(((3,4-Bis(octyloxy)phenyl)imino)methyl)-3-hydroxyphenyl 4-(dodecyloxy) benzoate **2a** (*n*=8). Yellow solid, yield 82%. ¹H NMR (CDCl₃): δ 0.85 (m, 9H, –CH₃, *J*=5.68 Hz), 1.28–1.34 (m, 32H, –CH₂), 1.46 (m, 6H, –CH₂), 1.82 (m, 6H, –CH₂), 4.01 (m, 6H, –OCH₂), 6.79 (d, 1H, Ar–H, *J*=8.01 Hz), 6.86 (m, 4H, Ar–H), 6.95 (d, 2H, Ar–H, *J*=8.88 Hz), 7.38 (d, 1H, Ar–H, *J*=8.43 Hz), 8.11 (d, 2H, Ar–H, *J*=8.8 Hz), 8.58 (s, 1H, –N=C–H), 13.77 (s, 1H, Ar–OH). ¹³C NMR (CDCl₃): δ 14.08, 14.17, 22.50, 22.72, 26.32, 28.28, 28.67, 30.02, 30.12, 30.38, 30.58, 30.62, 30.66, 30.68, 31.94, 69.32, 69.34, 69.62, 07.38, 110.5, 122.82, 114.15, 117.36, 121.78, 133.36, 133.80, 140.44, 149.57, 149.80, 154.63, 159.72, 162.52, 163.32, 164.85. Anal. Calcd for C₆₅H₉₄N₂O₆: C, 76.05; H, 9.44; N, 1.85. Found: C, 75.89; H, 9.15; N, 1.50.

4.8.3. (*E*)-4-(((3,4-Bis(decyloxy)phenyl)imino)methyl)-3-hydroxyphenyl 4-(dodecyloxy) benzoate **2a** (*n*=10). Yellow solid, yield 75%. ¹H NMR (CDCl₃): δ 0.87 (m, 9H, –CH₃), 1.25–1.34 (m, 40H, –CH₂), 1.48 (m, 6H, –CH₂), 1.82 (m, 6H, –CH₂), 4.03 (m, 6H, –OCH₂), 6.80 (d, 1H, Ar–H, *J*=8.57 Hz), 6.86 (m, 4H, Ar–H), 6.95 (d, 2H, Ar–H, *J*=8.82 Hz), 7.37 (d, 1H, Ar–H, *J*=8.44 Hz), 8.11 (d, 2H, Ar–H, *J*=8.80 Hz), 8.58 (s, 1H, –N=C–H), 13.76 (s, 1H, Ar–OH). ¹³C NMR (CDCl₃): δ 14.14, 22.71, 26.00, 29.11, 29.28, 29.33, 29.38, 29.45, 29.58, 29.61, 31.94, 37.69, 69.63, 107.40, 110.57, 112.98, 114.17, 117.25, 159.56, 162.49, 163.70, 164.40. Anal. Calcd for C₆₅H₉₄N₂O₆: C, 76.71; H, 9.78; N, 1.72. Found: C, 76.58; H, 9.75; N, 1.59.

4.8.4. (*E*)-4-(((3,4-Bis(tetradecyloxy)phenyl)imino)methyl)-3-hydroxyphenyl 4-(dodecyloxy)benzoate **2a** (*n*=14). Yellow solid, yield 86%. ¹H NMR (CDCl₃): δ 0.88 (m, 9H, –CH₃, *J*=5.75 Hz), 1.27–1.36 (m, 56H, –CH₂), 1.47 (m, 6H, –CH₂), 1.82 (m, 6H, –OCH₂), 4.03 (m, 6H, –OCH₂), 6.80 (d, 1H, Ar–H, *J*=8.35 Hz), 6.87 (m, 4H, Ar–H), 6.95 (d, 2H, Ar–H, *J*=8.74 Hz), 7.37 (d, 1H, Ar–H, *J*=8.45 Hz), 8.11 (d, 2H, Ar–H, *J*=8.73 Hz), 8.58 (s, 1H, –N=C–H), 13.76 (s, 1H, Ar–OH). ¹³C NMR (CDCl₃): 13.96, 22.60, 25.95, 26.04, 29.10, 29.36, 29.39, 29.49, 29.52, 29.58, 29.61, 29.65, 31.88, 68.41, 69.62, 69.89, 107.92, 110.51, 112.87, 113.12, 114.42, 114.82, 117.26, 121.48, 132.23, 132.69, 141.79, 148.84, 150.13, 154.71, 159.60, 163.73, 164.25. Anal. Calcd for C₆₅H₉₄N₂O₆: C, 77.79; H, 10.34; N, 1.51. Found: C, 77.64; H, 10.48; N, 1.46.

4.8.5. (*E*)-4-(((3,4-Bis(hexadecyloxy)phenyl)imino)methyl)-3-hydroxyphenyl 4-(dodecyloxy)benzoate **2a** (*n*=16). Yellow solid, yield 88%. ¹H NMR (CDCl₃): δ 0.86 (m, 9H, –CH₃), 1.24–1.34 (m, 64H, –CH₂), 1.46 (m, 6H, –CH₂), 1.80 (m, 6H, –CH₂), 4.01 (m, 6H, –OCH₂), 6.79 (d, 1H, Ar–H, *J*=8.51 Hz), 6.84 (m, 4H, Ar–H), 6.88 (d, 2H, Ar–H, *J*=8.35 Hz), 7.39 (d, 1H, Ar–H, *J*=8.50 Hz), 8.11 (d, 2H, Ar–H, *J*=8.89 Hz), 8.59 (s, 1H, –N=C–H), 13.77 (s, 1H, Ar–OH). ¹³C NMR (CDCl₃): δ 14.14, 22.71, 25.99, 26.05, 29.10, 29.27, 29.31, 29.37, 29.39, 29.46, 29.57, 29.60, 29.67, 29.69, 29.74, 31.94, 68.37, 69.36, 69.62,

107.38, 110.58, 112.96, 114.15, 114.35, 114.45, 117.26, 121.24, 132.38, 132.48, 132.79, 134.94, 141.44, 148.56, 149.80, 149.80, 154.53, 159.56, 162.49, 163.69, 164.44. Anal. Calcd for $C_{65}H_{94}N_2O_6$: C, 78.24; H, 10.57; N, 1.43. Found: C, 78.05; H, 10.44; N, 2.16.

4.9. Palladium complexes of (E)-4-(((3,4-bis(dodecyloxy)phenyl)imino)methyl)-3-hydroxyphenyl 6-(dodecyloxy)-2-naphthoate **1b** (n=12)

The mixture of 6-dodecyloxynaphthalene-2-carboxylic acid-4-[(3,4-didodecyloxyphenyl imino)methyl]-3-hydroxyphenyl ester (0.49 g, 5.11×10^{-4} mol) and $Pd(OAc)_2$ (0.054 g, 2.43×10^{-4} mol) dissolved in 25 mL absolute ethanol was refluxed for 24 h. The solution was concentrated under reduced pressure, and the products isolated as golden yellow solids were obtained after recrystallized from CH_2Cl_2/CH_3OH . Yield 81%. Anal. Calcd for $C_{120}H_{176}N_2O_{12}Pd$: C, 74.10; H, 9.03; N, Found: C, 74.26; H, 9.03. MS \ FAB: calcd for $[M]^+$, $C_{120}H_{176}N_2O_{12}Pd$, 1944.23; found 1944.23.

4.9.1. Palladium complex of (E)-4-(((3,4-dipropoxyphenyl)imino)methyl)-3-hydroxy phenyl 6-(dodecyloxy)-2-naphthoate **1b** (n=3). Yellow orange solid, yield 73%. Anal. Calcd for $C_{84}H_{104}N_2O_{12}Pd$: C, 70.06; H, 7.28; N, 1.95. Found: C, 69.99; H, 7.25; N, 1.32.

4.9.2. Palladium complex of (E)-4-(((3,4-bis(heptyloxy)phenyl)imino)methyl)-3-hydroxy phenyl 6-(dodecyloxy)-2-naphthoate **1b** (n=7). Yellow orange solid, yield 70%. Anal. Calcd for $C_{100}H_{136}N_2O_{12}Pd$: C, 72.15; H, 8.24; N, 1.68. Found: C, 71.12; H, 8.33; N, 2.34.

4.9.3. Palladium complex of (E)-4-(((3,4-bis(octyloxy)phenyl)imino)methyl)-3-hydroxy phenyl 6-(dodecyloxy)-2-naphthoate **1b** (n=8). Yellow orange solid, yield 65%. Anal. Calcd for $C_{104}H_{144}N_2O_{12}Pd$: C, 72.59; H, 8.44; N, 1.63. Found: C, 72.60; H, 8.55; N, 1.52.

4.9.4. Palladium complexes of (E)-4-(((3,4-bis(decyloxy)phenyl)imino)methyl)-3-hydroxyphenyl 6-(dodecyloxy)-2-naphthoate **1b** (n=10). Yellow orange solid, yield 69%. Anal. Calcd for $C_{112}H_{160}N_2O_{12}Pd$: C, 73.39; H, 8.80; N, 1.53. Found: C, 73.64; H, 9.05; N, 2.27.

4.9.5. Palladium complexes of (E)-4-(((3,4-bis(tetradecyloxy)phenyl)imino)methyl)-3-hydroxyphenyl 6-(dodecyloxy)-2-naphthoate **1b** (n=14). Yellow orange solid, yield 75%. Anal. Calcd for $C_{128}H_{192}N_2O_{12}Pd$: C, 74.73; H, 9.41; N, 1.36. Found: C, 75.04; H, 9.31; N, 2.18.

4.9.6. Palladium complexes of (E)-4-(((3,4-bis(hexadecyloxy)phenyl)imino)methyl)-3-hydroxyphenyl 6-(dodecyloxy)-2-naphthoate **1b** (n=16). Yellow orange solid, yield 77%. Anal. Calcd for $C_{136}H_{208}N_2O_{12}Pd$: C, 75.29; H, 9.66; N, 1.29. Found: C, 75.22; H, 9.62; N, 1.10.

4.10. Palladium complex of (E)-4-(((3,4-bis(dodecyloxy)phenyl)imino)methyl)-3-hydroxy phenyl 4-(dodecyloxy)benzoate **1a** (n=12)

Yellow orange solid, yield 80%. Anal. Calcd for $C_{112}H_{172}N_2O_{12}Pd$: C, 72.91; H, 9.40; N, Found: C, 72.63; H, 9.47. MS \ FAB: calcd for $[M]^+$, $C_{112}H_{172}N_2O_{12}Pd$, 1844.19; found 1844.21.

4.10.1. Palladium complex of (E)-4-(((3,4-dibutoxyphenyl)imino)methyl)-3-hydroxyphenyl 4-(dodecyloxy)benzoate **1a** (n=4). Yellow orange solid, yield 72%. Anal. Calcd for $C_{80}H_{108}N_2O_{12}Pd$: C, 68.82; H, 7.80. Found: C, 68.82; H, 7.49.

4.10.2. Palladium complex of (E)-4-(((3,4-bis(octyloxy)phenyl)imino)methyl)-3-hydroxy phenyl 4-(dodecyloxy)benzoate **1a** (n=8). Yellow orange solid, yield 72%. Anal. Calcd for $C_{96}H_{140}N_2O_{12}Pd$: C, 71.15; H, 8.71. Found: C, 70.69; H, 8.99.

4.10.3. Palladium complex of (E)-4-(((3,4-bis(decyloxy)phenyl)imino)methyl)-3-hydroxy phenyl 4-(dodecyloxy)benzoate **1a** (n=10). Yellow orange solid, yield 78%. Anal. Calcd for $C_{104}H_{156}N_2O_{12}Pd$: C, 72.09; H, 9.07. Found: C, 71.79; H, 9.22.

4.10.4. Palladium complex of (E)-4-(((3,4-bis(tetradecyloxy)phenyl)imino)methyl)-3-hydroxyphenyl 4-(dodecyloxy)benzoate **1a** (n=14). Yellow orange solid, yield 83%. Anal. Calcd for $C_{120}H_{188}N_2O_{12}Pd$: C, 73.64; H, 9.81. Found: C, 73.70; H, 9.80.

4.10.5. Palladium complex of (E)-4-(((3,4-bis(hexadecyloxy)phenyl)imino)methyl)-3-hydroxyphenyl 4-(dodecyloxy)benzoate **1a** (n=16). Yellow orange solid, yield 81%. Anal. Calcd for $C_{128}H_{204}N_2O_{12}Pd$: C, 74.29; H, 9.94. Found: C, 74.04; H, 9.81.

Acknowledgements

We thank the Ministry of Science and Technology, Taiwan, ROC (MOST 103-2113-M-008-002) for generous support of this work.

References and notes

- Donnio, B.; Guillon, D.; Deschenaux, R.; Bruce, D. W. In *Comprehensive Coordination Chemistry II*; McCleverty, J. A., Meyer, T. J., Eds.; Elsevier: Oxford (, 2003; pp 357–627.
- (a) Molochko, V. A.; Rukk, N. S. *Russ. J. Coord. Chem.* **2000**, *26*, 829–846; (b) Binnemans, K.; Gorller-Walrand, C. *Chem. Rev.* **2002**, *102*, 2303–2346; (c) Hoshino, N. *Coord. Chem. Rev.* **1998**, *174*, 77–108.
- Serrano, J. L. *Metallomesogens*; Wiley-VCH: Weinheim, 1996.
- (a) Bhattacharjee, C. R.; Das, G.; Mondal, P.; Prasad, S. K.; Rao, D. S. S. *Inorg. Chem. Commun.* **2011**, *14*, 606–612; (b) Bhattacharjee, C. R.; Das, G.; Mondal, P.; Prasad, S. K.; Rao, D. S. S. *Liq. Cryst.* **2011**, *38*, 615–623.
- (a) Mocanu, A. S.; Iliis, M.; Dumitrascu, F.; Ilie, M.; Circu, V. *Inorg. Chim. Acta* **2010**, *363*, 729–736; (b) Kadkin, O. N.; Kim, E. H.; Rha, Y. J.; Kim, S. Y.; Tae, J.; Choi, M. J. *Chem.—Eur. J.* **2009**, *15*, 10343–10347; (c) Rao, N. V. S.; Choudhury, T. D.; Paul, M. K.; Francis, T. *Liq. Cryst.* **2009**, *36*, 409–423; (d) Caruso, U.; Diana, R.; Panunzi, B.; Roviello, A.; Tingoli, M.; Tuzi, A. *Inorg. Chem. Commun.* **2009**, *12*, 1135–1141.
- Morale, F.; Finn, R. L.; Collinson, S. R.; Blake, A. J.; Wilson, C.; Bruce, D. W.; Guillon, D.; Donnio, B.; Schroder, M. *New J. Chem.* **2008**, *32*, 297–305.
- (a) Rezvani, Z.; Nejati, K.; Seyedahmadian, M.; Divband, B. *Mol. Cryst. Liq. Cryst.* **2008**, *493*, 71–81; (b) Hayami, S.; Motokawa, N.; Shuto, A.; Masuhara, N.; Someya, T.; Ogawa, Y.; Inoue, K.; Maeda, Y. *Inorg. Chem.* **2007**, *46*, 1789–1794.
- Rezvani, Z.; Divband, B.; Abbasi, A. R.; Nejati, K. *Polyhedron* **2006**, *25*, 1915–1920.
- (a) Wichmann, O.; Sillanpaa, R.; Lehtonen, A. *Coord. Chem. Rev.* **2012**, *256*, 371–392; (b) Evans, R. C.; Douglas, P.; Winscom, C. J. *Coord. Chem. Rev.* **2006**, *250*, 2093–2126; (c) Nejati, K.; Rezvani, Z. *New J. Chem.* **2003**, *27*, 1665–1669.
- (a) Perez Jubindo, M. A.; Rosario de la Fuente, M. *Adv. Mater.* **1994**, *6*, 941–944; (b) Serrano, J. L.; Romero, P.; Marcos, M.; Alonso, P. J. *J. Chem. Soc., Chem. Commun.* **1990**, *12*, 859–861.
- (a) Gupta, B. D.; Datta, C.; Das, C. D.; Bhattacharjee, C. R. *J. Mol. Struct.* **2014**, *1067*, 177–183; (b) Bhattacharjee, C. R.; Das, G.; Mondal, P. *J. Coord. Chem.* **2011**, *64*, 3273–3289.
- (a) Chakraborty, L.; Chakraborty, N.; Laskar, A. R.; Paul, M. K.; Rao, N. V. S. *J. Mol. Struct.* **2011**, *1002*, 135–144; (b) Jung, B. M.; Huang, Y. D.; Chang, J. Y. *Liq. Cryst.* **2010**, *37*, 85–92.
- Prajapati, A. K.; Bonde, N. *Liq. Cryst.* **2006**, *33*, 1189–1197.